ARL-TN-0921 ● Oct 2018

US Army Research Laboratory

Use of a High-Resolution WRF-ARW Ensemble to Provide Short-Range Guidance for a Complex Mixed Precipitation Event Near the Washington, DC, Area: Experimental Design

by Robert E Dumais Jr, Huaqing Cai, John Raby, and Brian Reen

NOTICES

Disclaimers

The findings in this report are not to be construed as an official Department of the Army position unless so designated by other authorized documents.

Citation of manufacturer's or trade names does not constitute an official endorsement or approval of the use thereof.

DESTRUCTION NOTICE—For classified documents, follow the procedures in DOD 5220.22-M, National Industrial Security Program Operating Manual, Chapter 5, Section 7, or DOD 5200.1-R, Information Security Program Regulation, C6.7. For unclassified, limited documents, destroy by any method that will prevent disclosure of contents or reconstruction of the document.

ARL-TN-0921 ● OCT 2018

US Army Research Laboratory

Use of a High-Resolution WRF-ARW Ensemble to Provide Short-Range Guidance for a Complex Mixed Precipitation Event Near the Washington, DC, Area: Experimental Design

by Robert E Dumais Jr, Huaqing Cai, John Raby, and Brian Reen
Computational and Information Sciences Directorate, ARL

REPORT DOCUMENTATION PAGE	*Form Approved* *OMB No. 0704-0188*

1. REPORT DATE *(DD-MM-YYYY)*	2. REPORT TYPE	3. DATES COVERED (From - To)
October 2018	Technical Note	9 February 2016–27 September 2018

4. TITLE AND SUBTITLE

Use of a High-Resolution WRF-ARW Ensemble to Provide Short-Range Guidance for a Complex Mixed Precipitation Event Near the Washington, DC, Area: Experimental Design

5a. CONTRACT NUMBER

5b. GRANT NUMBER

5c. PROGRAM ELEMENT NUMBER

6. AUTHOR(S)

Robert E Dumais Jr, Huaqing Cai, John Raby, and Brian Reen

5d. PROJECT NUMBER

5e. TASK NUMBER

5f. WORK UNIT NUMBER

7. PERFORMING ORGANIZATION NAME(S) AND ADDRESS(ES)

US Army Research Laboratory
ATTN: RDRL-CIE-M
White Sands Missile Range, NM 88002

8. PERFORMING ORGANIZATION REPORT NUMBER

ARL-TN-0921

9. SPONSORING/MONITORING AGENCY NAME(S) AND ADDRESS(ES)

10. SPONSOR/MONITOR'S ACRONYM(S)

11. SPONSOR/MONITOR'S REPORT NUMBER(S)

12. DISTRIBUTION/AVAILABILITY STATEMENT

Approved for public release; distribution is unlimited.

13. SUPPLEMENTARY NOTES

14. ABSTRACT

Using the Advanced Research version of the Weather Research and Forecast model, an ensemble of short-range weather forecasts were generated for a challenging winter precipitation forecast event near Washington, DC, on February 9, 2016. The motivation and design for this study case are explained, and initial results exploring 6-h precipitation forecasts are examined. Further verification work and plans for a follow-up paper are also discussed.

15. SUBJECT TERMS

mesoscale, ensemble, Weather Research and Forecast, WRF, precipitation, forecast, verification, uncertainty

16. SECURITY CLASSIFICATION OF:			17. LIMITATION OF ABSTRACT	18. NUMBER OF PAGES	19a. NAME OF RESPONSIBLE PERSON
					Robert E Dumais Jr
a. REPORT	b. ABSTRACT	c. THIS PAGE			19b. TELEPHONE NUMBER (Include area code)
Unclassified	Unclassified	Unclassified	UU	24	(575) 678-4650

Standard Form 298 (Rev. 8/98)
Prescribed by ANSI Std. Z39.18

Contents

Approved for public release; distribution is unlimited.

List of Figures

List of Tables

1. Introduction

The Washington, DC, area experienced a mixed winter precipitation event on the day of February 9, 2016, as a result of interactions between complex synoptic and mesoscale weather features. Trying to pinpoint where and when heavier mesoscale bands of precipitation might occur, in addition to forecasting the boundary layer temperature profiles and precipitation types, were the most challenging aspects of forecasting this event in the short term. The medium- to long-range forecasts also varied for days with respect to the synoptic flow evolution for this event. A wide array of global and limited-area mesoscale model forecasts provided a great variation of solutions for forecasters and planners to contemplate in days leading up to February 9. Even in the final 48 h prior to the event, global and mesoscale model ensemble forecasts had a wide degree of disagreement on not only mesoscale details of the evolving system, but also in the overlying synoptic details. The system eventually turned out to be a complex interaction of a Miller B-type (Miller 1946; Perry et al. 2007) winter system (with developing offshore coastal low), a large upper low and trough centered over the Great Lakes, several 500-mb short waves revolving around the upper trough, and a Norlun inverted trough structure (Zielinski 2009), which encouraged narrow mesoscale banding with localized enhanced vertical motion and precipitation (wherever it was interacting with the revolving short waves). In addition, a difficult to forecast borderline lower boundary layer temperature profile across the region created problems handling rain-versus-snow precipitation type in even the short-range forecasts. Slight warm air advection above about 925 mb was also an added feature contributing to precipitation type complexity. Enhanced areas of vertical motion and evaporative wet bulb temperature cooling potential could better support snow versus rain, and was somewhat transient throughout the forecast period. In general, snow was favored well north and especially northwest of the DC metro area, while rain was more favored to the south and over the DelMarva Peninsula. Heavier snow bands to the north supported some accumulation, while other places saw only slushy brief accumulations on just grassy surfaces.

Because of the high level of uncertainty in model forecasts leading up to the day of this event, although resultant winter precipitation impacts were not widespread (mainly in sectors such as NW Maryland and near the Pennsylvania state line), there were still significant headaches created for local decision makers in the antecedent days and hours (Samenow and Junker 2016). Less-intense winter weather systems often can be challenging to forecasters, and this is especially true when precipitation is anticipated within surface and boundary layer temperature profiles hovering around where multiple winter precipitation types can be supported. In addition, preexisting ground temperatures can either be supportive or nonsupportive of rapid accumulation of frozen precipitation early in the event. For example, snow may only accumulate during heavier bursts over grassy surfaces. Continued difficulties in short-range forecasting of such winter events can still adversely impact military as well as civilian operational planning decisions.

We designed an experiment consisting of many different model forecast simulations (known as a model ensemble) for this winter case study event, applying a high-resolution triple-nest implementation of the Advanced Research version of the Weather Research and Forecast model (WRF-ARW, but referred to as just WRF hereafter) in a configuration similar to that tested as a prototype US Army Research Laboratory (ARL) Weather Running Estimate-Nowcast (WRE-N) system (Dumais et al. 2013). The WRF is discussed in detail by Skamarock et al. (2008). The WRE-N focuses on the 0–6 h "nowcast" period, which is also the forecast lead period of interest for our study. The ensemble forecast results are now undergoing analysis and verification to better understand how WRE-N nowcasts in the future might be applied more intelligently toward addressing short-range forecast uncertainty, which in turn would provide information of greater "value added" to both military and civilian decision makers. We also explore the impact of model spatial resolution via nesting on these forecasts.

2. WRE-N Configuration for the Case Study

The WRE-N is an ARL implementation of the WRF model developed by the National Center for Atmospheric Research (NCAR) and other contributors from within the numerical weather modeling community (Skamarock et al. 2008), and it also employs the WRF four-dimensional data assimilation (FDDA) observation nudging option to incorporate regional and local direct weather observations when available (Dumais et al. 2013). As applied in this study, 6 h of "preforecast" FDDA were used to allow the model to "spin up" mesoscale dynamics and achieve balance while also incorporating the most recent observational data. After this period, the model was allowed to free forecast for another 12 h. The initial 6 h of the 12-h free forecast period will be the focus of an upcoming paper to be drafted after completion of the ongoing analysis and verification, since it is really the main focus forecast lead time of the WRE-N.

The model was centered at 39.032° N and 76.952° W, and was telescopically nested (Fig. 1) in a hierarchy of three horizontal resolutions: 9 km, 3 km, and 1 km grid spacing. The outer 9-km nest was dimensioned at 279 × 279, covering an areal extent of 2502 km × 2502 km. The middle 3-km nest used 241 × 241 dimensions covering 720 km × 720 km, and the inner 1-km nest used 205 × 205 dimensions covering 204 km × 204 km. This nesting paradigm is consistent with how ARL envisions that the Army might run WRE-N in a nowcast cycling mode as a forward echelon application. It provides for a reasonable outer mesh size and resolution for nesting from operational global model forecasts, and also a fine enough inner nest resolution for resolving individual convective storms and many other important types of complex terrain flows that can impact the Army. A Lambert conformal map projection was used for the simulation. All model simulations were run from 2016 0600 UTC 09 Feb–0000 UTC 10 Feb, with model output written out at hourly forecast intervals.

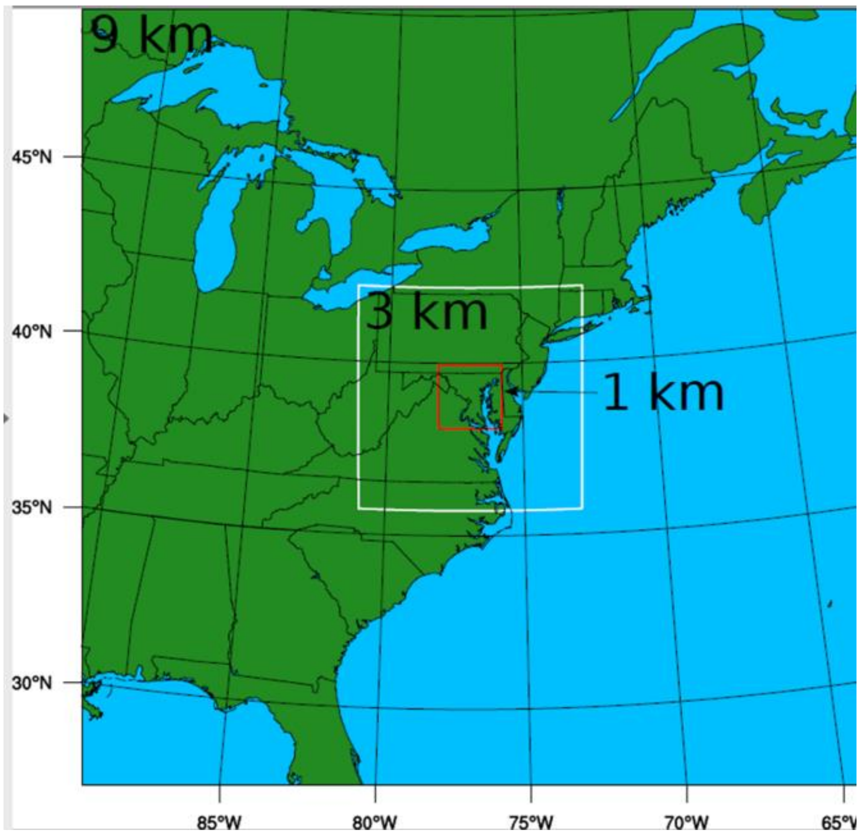

Fig. 1 WRF model nest domains used in study

An ensemble of WRF model simulations, although not practical to execute in a real-time forward echelon modeling environment in the near future, is targeted in this study for developing improved understanding of how model mesoscale forecast uncertainty can still hinder decision makers at short lead times. A relatively simple ensemble was created for this purpose, using a membership differing mostly in terms of physics (microphysics, radiation, boundary layer turbulence, cumulus parameterization) options, dynamics options, diffusion/advection options, choice of external operational global/regional model used for nest 1 first guess/lateral boundary conditions, and whether or not FDDA was applied. This construct of a combination physics and mixed model ensemble has been shown in some instances to be beneficial for short-range mesoscale model forecasting, especially under weak synoptic forcing (Stensrud et al. 2000; Eckel and Mass 2005). They are also easier and less complex to produce than typical initial condition perturbed ensembles produced at global centers, although more recently stochastic ensemble approaches have also gained traction. Here, the possible options for an external operational model to use for initializing and providing time-dependent lateral boundary conditions (for the outer 9-km nest) of ensemble members were either from the National Center for Environmental Prediction (NCEP) deterministic Global Forecast System (GFS) 0.5° cycle based at 0600 UTC 09 Feb, the NCEP Global Ensemble Forecast System (GEFS) 0.5° ensemble model cycle based at 0600 UTC 09 Feb, or the NCEP mesoscale North American Model (NAM) deterministic model cycle based at 0600 UTC 09 Feb.

The various WRF ensembles were all variants from a single "base" model configuration of physics and dynamics options. Table 1 describes the base configuration settings.

Table 1 Baseline physics/dynamics settings for WRF v 3.6.1 experiments

Grid spacing for each nest: 9 km, 3 km, 1 km
Number of vertical terrain-following levels: 57
Advective time step = 27 s for nest 1 (reduced by a ratio of 3:1 for each successive nest)
Mellor–Yamada–Janjić (MYJ) planetary boundary layer physics: bl_pbl_physics=2.
Eta model surface layer similarity physics: sf_sfclay_physics=2.
Noah land surface physics: sf_surface_physics=2.
Dudhia short wave radiation parameterization: ra_sw_physics=1 with swint_opt=1.
Rapid Radiative Transfer Model (RRTM) long-wave radiation parameterization: ra_lw_physics=1
Slope and shadow effects for solar radiation at surface: slope_rad=1, topo_shading=1, shadlen=15000.
Grell–Freitas scale-aware ensemble deep cumulus convection physics (with shallow cumulus option turned on) as well as cu_rad_feedback: cu_physics=3, ishallow=1, cu_rad_feedback=.true., all nests.
Vertical damping option 3 (w-Rayleigh) turned on with 5-km damping zone from model top of 50 mb: damp_opt=3, dampcoeff=0.2, zdamp=5000.
Horizontal Smagorinsky turbulent diffusion option on Cartesian surfaces: diff_opt=2, km_opt=4.
6th-order numerical diffusion filter: diff_6th_opt=2; diff_6th_factor=0.12.
United States Geological Survey (USGS) 24 category land use: 30 arc sec resolution
State Soil Geographic (STATSGO) 16 category soil texture: 30 arc sec resolution
USGS GTOPO 30 arc sec terrain elevation
W_damping=1
Thompson microphysics: mp_physics=8.
epssm= 0.5 for all nests.
Obs_nudge_opt=1 for all nests (FDDA observation nudging turned on)
Advection schemes: 5th (horizontal) and 3rd (vertical) order
Two-way nest feedback: off (feedback=0)

Starting with the base namelist configuration listed in Table 1, the various ensemble members vary in 1) physics/dynamics/diffusion namelist options as presented in Table 1, 2) the external model providing initial and lateral boundary conditions for the outer 9-km nest, 3) the available temporal frequency of external model lateral boundary conditions, and 4) whether observation nudging FDDA was applied (which was just for one of the members—all others did not use FDDA). The various 28 ensemble members are described in Table 2.

Table 2 The 28 WRF ensemble members used in study. All of these assume the namelist physics/dynamics (base) from Table 1 unless a particular change in a package or option is noted in the change phys/dyns column.

Change phys/dyns	External model for initial and lateral boundary conditions	Forecast interval frequency of external model GRIB files	FDDA	Ensemble member name
base	GFS ½ deg	3 h	yes	E1
base	NAM 218	1 h	yes	E2
base	GEFS ½ deg (ctrl)	6 h	yes	E3
base	GEFS ½ deg (#1)	6 h	yes	E4
base	GEFS ½ deg (#4)	6 h	yes	E5
base	GEFS ½ deg (#5)	6 h	yes	E6
base	GEFS ½ deg (#9)	6 h	yes	E7
base	GEFS ½ deg (#10)	6 h	yes	E8
base	GEFS ½ deg (#11)	6 h	yes	E9
base	GEFS ½ deg (#16)	6 h	yes	E10
base	NAM 218	3 h	yes	E11
base	NAM 218	6 h	yes	E12
base	GFS ½ deg	6 h	yes	E13
Mellor–Yamada–Nakanishi–Niino (MYNN) 2.5 planetary boundary and surface layer	NAM 218	1 h	yes	E14
Yonsei State University (YSU) planetary boundary and MM5 surface layer	NAM 218	1 h	yes	E15
Quasi-Normal Scale Elimination (QNSE) planetary boundary and surface layer	NAM 218	1 h	yes	E16
BouLac planetary boundary and Eta surface layer	NAM 218	1 h	yes	E17
RRTM for GCMs (RRTM-G) short/long wave radiation and Thompson aerosol-aware microphysics	NAM 218	1h	yes	E18
New Goddard short-/long-wave radiation	NAM 218	1 h	yes	E19
Lin microphysics	NAM 218	1 h	yes	E20
WRF Single Moment 5-Class (WSM5) microphysics	NAM 218	1 h	yes	E21
Morrison microphysics	NAM 218	1 h	yes	E22
Kain–Fritsch cumulus on nest 1	NAM 218	1 h	yes	E23
diff_opt=1; km_opt=4 for horizontal Smagorinsky turbulent diffusion on model terrain-following surface	NAM 218	1 h	yes	E24
diff_opt_6th= 0	NAM 218	1 h	yes	E25
4th-order horizontal and 2nd-order vertical advection	NAM 218	1 h	yes	E26
Two-way nest feedback (feedback=1)	NAM 218	1 h	yes	E27
base	NAM 218	1 h	no	E28

The NAM is the current operational limited-area mesoscale model used by the NCEP, and is really an implementation of the NCEP nonhydrostatic multiscale model on the B grid (NMMB) described in Janjić and Gall (2012). It is distributed by NCEP on a 12-km resolution grid referred to as the "218 grid", and for this study "NAM 218" refers to this. It runs at a frequency of four cycles per day (12, 18, 00, and 06 UTC). The global model run at NCEP is called the GFS (Sela 2009). The study here used half-degree resolution GFS model output. As with the NAM, it is also run operationally at a frequency of four cycles per day (same times as listed for NAM). The NCEP offers NAM output files in forecast intervals as fine as hourly, while the GFS offers intervals only as fine as every 3 h. The GEFS is an ensemble of 21 different GFS forecast members (Zhou et al. 2017), which was also available for this study at half-degree resolution. It too is run operationally at the same four cycle hours as NAM and GFS by NCEP. Only a subset of these 21 GEFS members, selected subjectively prior to the study, were used to generate WRF ensemble members in our study (see Table 2). The temporal frequency for GEFS output files was just 6 h. For land use classification and soil texture initialization, the United States Geological Survey (USGS) 24-category global 30-arc second dataset (Gesch and Larson 1996) along with the State Soil Geographic (STATSGO) 16-class 30 arc second data set (USDA 1994) were used. For terrain elevation, the 30 arc second resolution USGS GTOPO30 data set was used (Gesch and Larson 1996).

Table 3 Options in WRF referred to in Tables 1 and 2

MYJ planetary boundary layer scheme	Janjić 1994
Eta surface layer similarity scheme	Janjić 2002
YSU planetary boundary layer scheme	Hong et al. 2006
MM5 surface layer similarity scheme	Beljaars 1994
MYNN Level 2.5 planetary boundary layer scheme	Nakanishi and Niino 2009
MYNN surface layer scheme	Nakanishi and Niino 2009
QNSE planetary boundary layer scheme	Sukoriansky et al. 2005
QNSE surface layer scheme	Sukoriansky et al. 2005
Bougeault–Lacarrère (BouLac) planetary boundary layer scheme	Bougeault and Lacarrère 1989
RRTMG short-wave and long-wave radiation schemes	Iacono et al. 2008
Dudhia short-wave radiation scheme	Dudhia 1989

New Goddard short wave and long wave radiation schemes	Chou and Saurez 1999; Chou et al. 2001
Lin microphysics scheme	Lin et al. 1983
WSM5 microphysics scheme	Hong et al. 2004
Morrison 2-moment microphysics scheme	Morrison et al. 2009
Thompson Aerosol-aware microphysics scheme	Thompson and Eidhammer 2014
Kain–Fritsch Deep Cumulus scheme (includes shallow cumulus treatment)	Kain 2004
Grell–Freitas Scale and Aerosol-aware Deep ensemble Cumulus scheme (with shallow cumulus treatment)	Grell and Freitas 2014
Unified Noah Land Surface Model	Tewari et al. 2004
epssm (This is a sound-wave damper/time step offset that can stabilize steep slope treatment by dynamics (little other effect)	Dudhia 1995
6th-order numerical diffusion filter	Knievel et al. 2007
Smagorinsky 2-D horizontal turbulent diffusion	Smagorinsky 1963
Implicit Rayleigh damping for vertical velocity	Klemp et al. 2008

3. Conclusion and Summary Discussion

The simulations were completed successfully using a local ARL Powerwulf Linux cluster, and some initial results are displayed a bit later. The primary focuses for subsequent verification efforts will be aimed at 1) impact of choice of model physics/dynamics/advection options on the subsequent evolution of short-range surface and precipitation field forecasts for this event; 2) impact of choice of synoptic conditions (via different global model solutions for applying lateral boundary conditions) for the same; and 3) the impact of the different model resolutions for the same. Besides use of more conventional statistical verification methods (such as bias, root mean square-error, and correlation coefficient) for evaluating forecast accuracy, this study will also allow for different metrics more appropriate for precipitation such as the fractional skill score (FSS). The FSS is a useful measure of the spatial accuracy of quantitative precipitation forecasts. The papers of Mittermaier and Roberts (2010), as well as Cai and Dumais (2015), discuss and illustrate some of the value of using spatial verification techniques such as FSS for precipitation, versus traditional point verification methods. This is especially true for higher-resolution numerical weather prediction (NWP) where small spatial and temporal displacement errors can provide misleading information about forecast performance, and also with the use of radar-derived precipitation estimates for ground truth. In the case of this study, NCEP's hourly Stage IV Quantitative Precipitation Estimate national mosaic (4-km grid spacing) dataset is used for verification ground truth (Nelson et al. 2016). The forecasts from the model grids are first interpolated onto a destaggered grid (from WRF native staggered C grid), although at the same horizontal grid spacing as the WRF native input grid. This is done using the NCAR Unified Post Processor (UPP; https://dtcenter.org/upp/users/docs/user_guide/V3/upp_users_guide.pdf). The UPP software also interpolates the WRF output onto pressure surfaces (from native sigma), computes all additional variables of interest from WRF basic prognostic variables, and generates additional diagnostic levels where the NCAR Model Evaluation Tools (MET; https://dtcenter.org/met/users/index.php) is designed to do its model verification computations. The final step of regridding the model precipitation fields onto the 4-km Stage IV observation grid was accomplished (after the UPP step) via the MET software package called "Ensemble-Stat". The additional MET software called Grid-Stat can be used for producing fields needed for calculating FSS.

Although the results from the verification portion of this study are ongoing and will be published at a later date, a subjective preliminary examination of quantitative precipitation fields produced by the 1-km WRF nest indicates that the choice of global or regional operational model used to provide lateral boundary conditions may have had more impact to short-range forecasts in this case than choice of WRF physics/dynamics/advection options. These results will be processed further and shown in a later report. Figures 2 through 4 illustrate that the main WRF ensemble mean precipitation structure appeared to be captured reasonably well, but displaced to the north, although certain individual ensemble members did handle the spatial and temporal features of the precipitation structures better. Future analysis will provide more details to expand upon this initial thought, and also consider other surface fields than just precipitation. These also will be discussed in a later report.

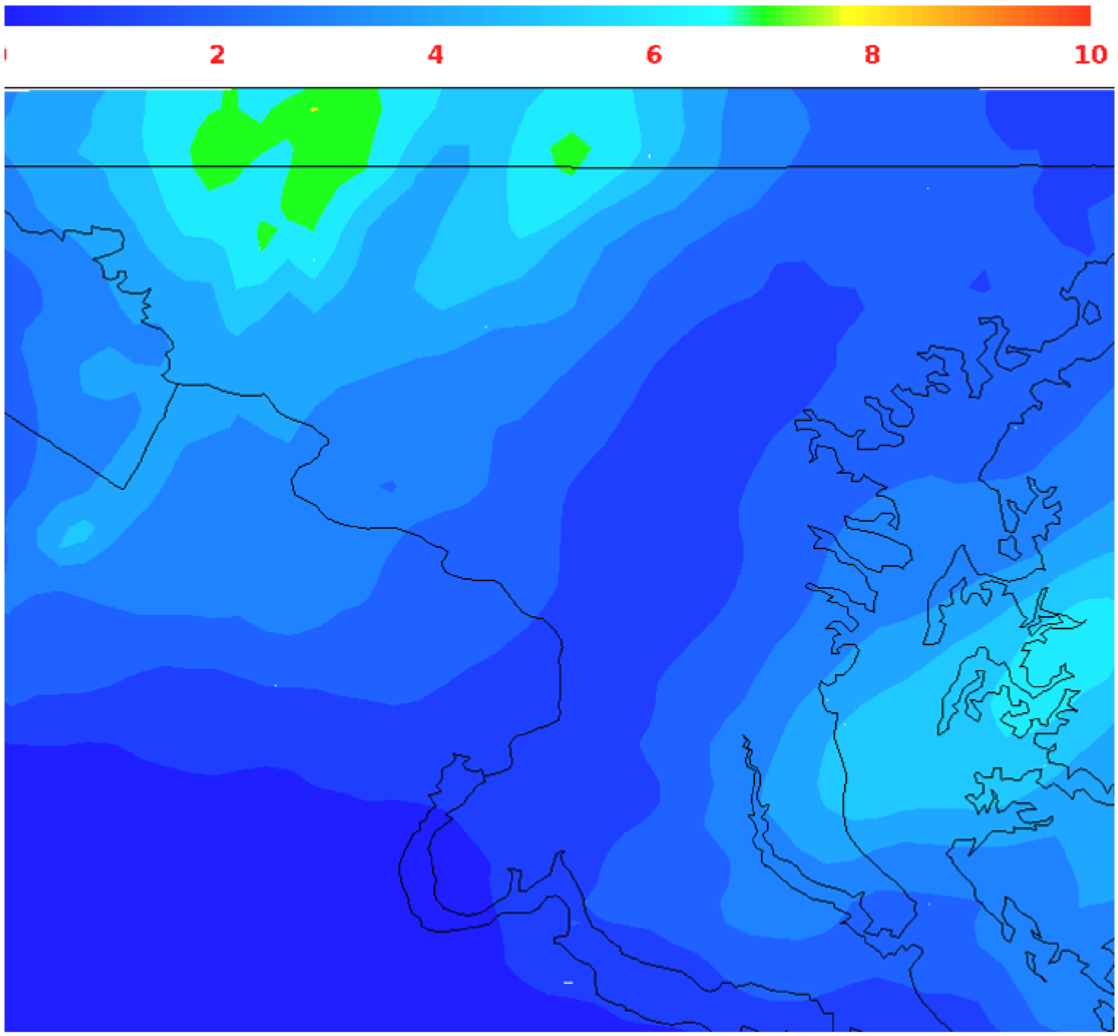

Fig. 2 WRF ensemble mean 6-h accumulated precipitation (mm) for period 12–18 UTC 09 Feb

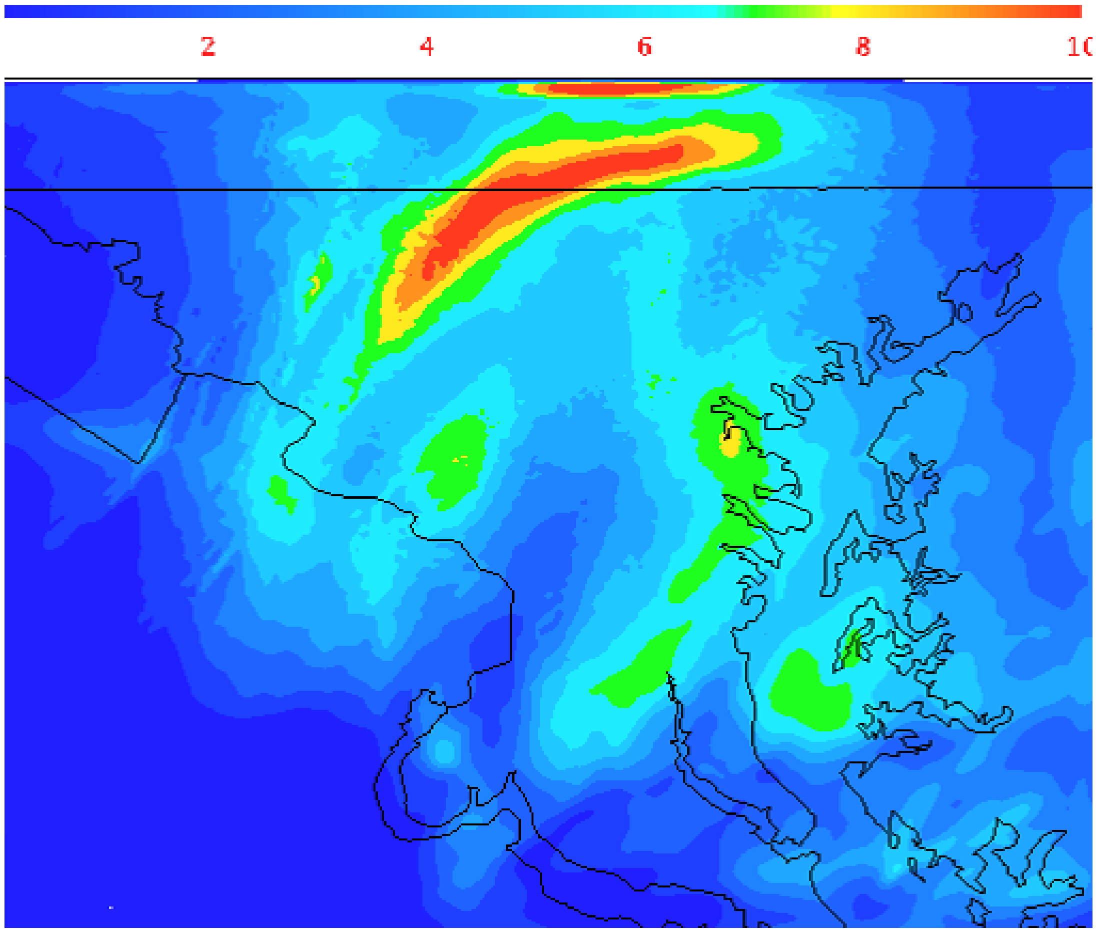

Fig. 3 WRF ensemble member #6 6-h accumulated precipitation (mm) for period 12–18 UTC 09 Feb

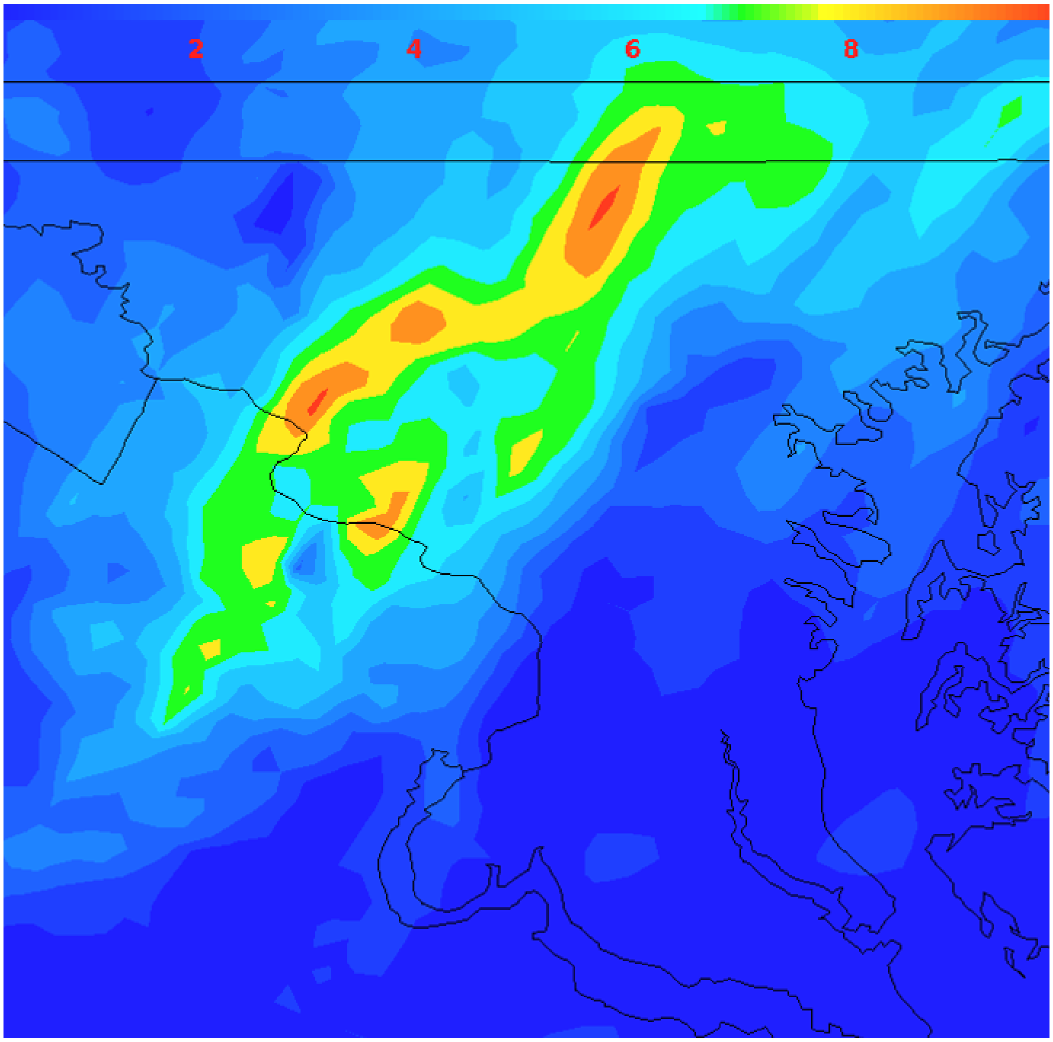

Fig. 4 **Stage IV observed 6-h accumulated precipitation (mm) for period 12–18 UTC 09 Feb**

Approved for public release; distribution is unlimited.

4. References

Beljaars ACM. The parameterization of surface fluxes in large-scale models under free convection. Q J R Meteorol Soc. 1994;121:255–270.

Bougeault P, Lacarrère P. Parametrization of orography-induced turbulence in a mesobeta-scale model. Mon Wea Rev. 1989;117:1872–1890.

Cai H, Dumais RE. Object-based evaluation of a numerical weather prediction model's performance through storm characteristic analysis. Weather and Forecasting. 2015;30:1451–1468.

Chou MD, Suarez MJ. A solar radiation parameterization for atmospheric studies. Washington (DC): NASA; 1999. Report No.: 104606, 40.

Chou MD, Suarez MJ, Liang XZ, Yan MMH. A thermal infrared radiation parameterization for atmospheric studies. Washington (DC): NASA; 2001. Report No.: 104606, 19.

Dudhia J. Numerical study of convection observed during the winter monsoon experiment using a mesoscale two-dimensional model. J Atmos Sci. 1989;46:3077–3107.

Dudhia J. Reply. Mon. Wea. Rev. 1995;123:2573–2575.

Dumais Jr RE, Kirby SF, Passner JE, Knapp DI. Development of a nowcast modeling system to support Army aviation forecasts. The 16th Conference on Aviation, Range, and Aerospace Meteorology, 93rd Annual American Meteorological Society Conference; 2013 Jan 6–10; Austin, TX.

Eckel FA, Mass CF. Effective mesoscale, short-range ensemble forecasting. Weather and Forecasting. 2005;20:3238–350

Gesch DB, Larson KS. Techniques for development of global 1-kilometer digital elevation models. Pecora Thirteen, Human Interactions with the Environment – Perspectives from Space; 1996 Aug 20–22; Sioux Falls, SD.

Grell GA, Freitas SR. A scale and aerosol aware stochastic convective parameterization for weather and air quality modeling, Atmos Chem Phys. 2014;14:5233–5250.

Hong S–Y, Dudhia J, Chen S–H. A revised approach to ice microphysical processes for the bulk parameterization of clouds and precipitation. Mon Wea Rev. 2004;132:103–120.

Hong SY, Noh Y, Dudhia J. A new vertical diffusion package with an explicit treatment of entrainment processes. Mon Wea Rev. 2006;134:2318–2341.

Iacono MJ, Delamere JS, Mlawer EJ, Shephard MW, Clough SA, Collins WD. Radiative forcing by long–lived greenhouse gases: calculations with the AER radiative transfer models. J Geophys Res. 2008;113:D13103.

Janjić ZI. The step–mountain eta coordinate model: further developments of the convection, viscous sublayer and turbulence closure schemes. Mon Wea Rev. 1994;122:927–945.

Janjić ZI. Nonsingular implementation of the Mellor-Yamada level 2.5 scheme in the NCEP meso model. College Park (MD): NCEP; 2002. Report No.: 437.

Janjić ZI, Gall R. Scientific documentation of the NCEP nonhydrostatic multiscale model on the B grid(NMMB), part 1 dynamics. Boulder (CO): NCAR; 2012. Report No.: NCAR/TN-489+STR. doi:10.5065/D6WH2MZX,.

Kain JS. The Kain–Fritsch convective parameterization: an update. J Appl Meteor. 2004;43:170–181.

Klemp JB, Dudhia J, Hassiotis AD. An upper gravity-wave absorbing layer for NWP applications. Mon Wea Rev. 2008; doi: 10.1175/2008MWR2596.1.

Knievel JC, Bryan GH, Hacker JP. Explicit numerical diffusion in the WRF Model. Mon Wea Rev. 2007;135:3808–3824.

Lin Y-L, Farley RD, Orville HD. Bulk parameterization of the snow field in a cloud model, J Clim Appl Meteorol., 1983;22:1065–1092.

Miller JE. Cyclogenesis in the Atlantic Coastal region of the United States. J Meteor. 1946;3:31–44.

Mittermaier MP, Roberts N. Inter-comparison of spatial forecast verification methods: identifying skillful spatial scales using the fractions skill score. Weather and Forecasting. 2010;25:343–354.

Morrison H, Thompson G, Tatarskii V.: Impact of cloud microphysics on the development of trailing stratiform precipitation in a simulated squall line: comparison of one- and two-moment schemes. Mon Wea Rev. 2009;137:991–1007.

Nakanishi M, Niino H. Development of an improved turbulence closure model for the atmospheric boundary layer. J Meteor Soc Japan. 2009;87:895–912, doi:10.2151/jmsj.87.895.

Nelson BR, Prat OP, Seo D-J, Habib E. Assessment and implications of NCEP stage IV quantitative precipitation estimates for product intercomparisons. Weather and Forecasting. 2016;31:371–394.

Perry B, Konrad CE, Hotz D, Lee LG. Synoptic classification of snowfall events in the Great Smoky Mountains, USA. 64th Eastern Snow Conference; 2007; St. Johns, Newfoundland, Canada.

Samenow J, Junker W. Snowy tonight and Tuesday; accumulation forecast extremely difficult. Washington (DC): The Washington Post; 2016 Feb 8 [accessed 2018 Oct 1]. https://www.washingtonpost.com/news/capital-weather-gang/wp/2016/02/08/snowy-tonight-and-tuesday-accumulation-forecast-extremely-difficult/?utm_term=.f9324c0530af.

Sela J. Implementation of the sigma pressure hybrid coordinate into GFS. College Park (MD): NCEP; 2009. Report No.: 461.

Skamarock WC, Klemp JB, Dudhia J, Gill DO, Barker DM, Duda MG, Huang X-Y, Wang W, Powers JG. A description of the advanced research WRF version 3. Boulder (CO): NCAR; 2008. Report No.: NCAR/TN-4751STR.

Smagorinsky J. General circulation experiments with the primitive equations. Mon Wea Rev. 1963;91:99–164.

Stensrud DJ, Bao J-W, Warner TT. Using initial condition and model physics perturbations in short-range ensemble simulations of mesoscale convective systems. Mon Wea Rev. 2000;128:2077–2107.

Sukoriansky S, Galperin B, Perov V. Application of a new spectral theory of stably stratified turbulence to the atmospheric boundary layer over sea ice. Bound-Layer Meteor. 2005; 117:231–257.

Tewari M, Chen F, Wang W, Dudhia J, LeMone MA, Mitchell K, Ek M, Gayno G, Wegiel J, Cuenca RH. 2004: Implementation and verification of the unified NOAH land surface model in the WRF model. 20th Conference on Weather Analysis and Forecasting/16th Conference on Numerical Weather Prediction, 84th Annual American Meteorological Society Meeting; 2004 Jan 11–15; Seattle, WA. p. 11–15.

Thompson G, Eidhammer T. A study of aerosol impacts on clouds and precipitation development in a large winter cyclone. J Atmos Sci. 2014;71.10:3636–3658.

US Department of Agriculture. State Soil Geographic (STATSGO) data base: data use information. Soil Conserv Serv; 1994.

Zielinski G. Conditions may vary: A guide to Maine weather. Camden (ME): Down East Books; 2009.

Zhou X, Zhu Y, Hou D, Luo Y, Peng J, Wobus R. Performance of the new NCEP global ensemble forecast system in a parallel experiment. Weather and Forecasting. 2017. doi:10.1175/WAF-D-17-0023.1.

List of Symbols, Abbreviations, and Acronyms

ARL	US Army Research Laboratory
BouLac	Bougeault–Lacarrère
FDDA	four-dimensional data assimilation
FSS	fractional skill score
GEFS	Global Ensemble Forecast System
GFS	Global Forecast System
MET	Model Evaluation Tools
MYJ	Mellor–Yamada–Janjić
MYNN	Mellor–Yamada–Nakanishi–Niino
NAM	North American Model
NCAR	National Center for Atmospheric Research
NCEP	National Center for Environmental Prediction
NMMB	nonhydrostatic multiscale model on the B grid
NWP	numerical weather prediction
QNSE	Quasi-Normal Scale Elimination
RRTM	Rapid Radiative Transfer Model
RRTM-G	RRTM for GCMs
STATSGO	State Soil Geographic
UPP	Unified Post Processor
USGS	United States Geological Survey
WRE-N	Weather Running Estimate-Nowcast
WRF-ARW	Weather Research and Forecast model
WSM5	WRF Single Moment 5-Class
YSU	Yonsei University

1 (PDF)	DEFENSE TECHNICAL INFORMATION CTR DTIC OCA
2 (PDF)	DIR ARL IMAL HRA RECORDS MGMT RDRL DCL TECH LIB
1 (PDF)	ARL RDRL CIE M R DUMAIS